

---

# FUSFORMER: A TRANSFORMER-BASED FUSION APPROACH FOR HYPERSPECTRAL IMAGE SUPER-RESOLUTION

---

A PREPRINT

**Jin-Fan Hu**

School of Mathematical Sciences  
University of Electronic Science and Technology of China  
Chengdu, 611731, China  
hujf0206@163.com

**Ting-Zhu Huang**

School of Mathematical Sciences  
University of Electronic Science and Technology of China  
Chengdu, 611731, China  
tingzhuhuang@126.com

**Liang-Jian Deng**

School of Mathematical Sciences  
University of Electronic Science and Technology of China  
Chengdu, 611731, China  
liangjian.deng@uestc.edu.cn

September 7, 2021

## ABSTRACT

Hyperspectral image has become increasingly crucial due to its abundant spectral information. However, It has poor spatial resolution with the limitation of the current imaging mechanism. Nowadays, many convolutional neural networks have been proposed for the hyperspectral image super-resolution problem. However, convolutional neural network (CNN) based methods only consider the local information instead of the global one with the limited kernel size of receptive field in the convolution operation. In this paper, we design a network based on the transformer for fusing the low-resolution hyperspectral images and high-resolution multispectral images to obtain the high-resolution hyperspectral images. Thanks to the representing ability of the transformer, our approach is able to explore the intrinsic relationships of features globally. Furthermore, considering the LR-HSIs hold the main spectral structure, the network focuses on the spatial detail estimation releasing from the burden of reconstructing the whole data. It reduces the mapping space of the proposed network, which enhances the final performance. Various experiments and quality indexes show our approach's superiority compared with other state-of-the-art methods.

**Keywords** Hyperspectral image super-resolution, Image fusion, Transformer

## 1 Introduction

Hyperspectral images have recently received a lot of attention in many fields since the rich spectral information of each pixel in a scenario provides more abundant and reliable knowledge than those multispectral images (e.g., RGB images). As a result, many researchers start taking advantage of the characteristics of HSI in various computer vision tasks, such as classification, segmentation, and object tracking begin the HSIs for better performance. However, limited by the current physical imaging system, there is an unavoidable trade-off, the high spatial resolution and high spectral

resolution cannot be obtained at the same time [1]. The imaging mechanism can only capture the image with high spatial resolution along with limited spectral bands, e.g., high-resolution multispectral image (HR-MSI), or low spatial resolution but with a higher spectral resolution, e.g., low-resolution hyperspectral image (LR-HSI) in practice. Thus, Fusing the high spatial resolution of MSI and high spectral resolution of HSI becomes a promising technique to generate the desired high-resolution hyperspectral image (HR-HSI).

Many methods have been proposed from various perspectives to address the HSI super-resolution problem in the last few years. They are roughly divided into two classes: traditional methods and deep learning-based methods. As for the traditional methods, many researchers introduce different prior knowledge in their proposed optimization models for exploiting the intrinsic properties under the maximum a posteriori (MAP) framework.

Since matrix or tensor factorization-based methods show reliable and promising performance in many computer vision and image processing tasks [2, 3, 4, 5], many researchers also introduce the matrix or tensor factorization methodology into the hyperspectral image super-resolution or pansharpening problems [6, 7, 8, 9, 10, 11, 12, 13, 14, 15, 16, 17, 18]. Although those methods have achieved excellent performance, they often require known or estimated  $\mathbf{B}$  and  $\mathbf{R}$  beforehand, which are difficult to obtain in practice. Furthermore, the representation ability of those handcraft regularization terms is usually limited in actual life, and their optimal parameters need to be tuned for different devices.

Recently, deep learning-based methods have shown satisfactory performance in different fields due to their remarkable feature representing ability. Thus, many researchers take the deep learning, especially the CNN technique into consideration for fusing the LR-HSI and HR-MSI [19, 20, 21, 22, 23, 24, 25, 26, 27, 10, 28, 29] which have outperformed many traditional methods. Nevertheless, due to its insufficient information extraction ability of convolution, there is still room for improvement.

In this work, we notice that the transformer and its various modifications have obtained outstanding achievements in natural language processing and computer vision tasks [30, 31, 32]. Hence, a transformer-based network architecture called Fusformer is proposed for the hyperspectral image super-resolution problem. Our method integrates a self-attention mechanism that can exploit more global relationships among the data than the convolution operation with a limited receptive field. Furthermore, we force our Fusformer to estimate the residuals instead of reconstructing the whole HR-HSI, enabling the network architecture to learn in a smaller mapping space. This paper designs an efficient network architecture to solve the HSI super-resolution problem via fusing the HR-MSI and LR-HSI. To sum up, the contributions of this paper are presented as follows:

1. To our knowledge, it is the first time using the transformer to solve the hyperspectral image super-resolution problem. The self-attention mechanism in the transformer enables our network to represent more global information than previous CNN architectures.
2. The proposed approach focuses on the residual domain instead of the primitive image domain, which leads to a smaller mapping space. It relieves the network of the burden of reconstructing the desired HR-HSI directly.
3. Only a few parameters are involved in the network with light computation making our approach practical in the real-life application. Furthermore, the network is plain and easy to follow. Thus, future researches can be improved based on our simple yet effective architecture.

The organization of this article is as follows. Section II will introduce our Fusformer architecture in detail. In Section III, extensive experiments on different datasets are presented to validate the superiority of our network. Finally, we draw the conclusion in Section IV. In this paper, we utilize non-bold case, bold upper case, and calligraphic upper case letters to denote the scalar, matrix, tensor, respectively.

## 2 Network Architecture

With the rapid development of deep learning techniques, CNN-based approaches are also used for solving many tasks of computer vision and image processing, including the pansharpening and the HSI-MSI fusion problem [19, 20, 21, 22, 23, 24, 25, 26, 27, 10, 28, 29]. They have obtained state-of-the-art performance in recent years due to their powerful feature extraction ability. Notwithstanding the remarkable achievements of those CNN-based methods have obtained, the core elements in the neural network are those various convolution kernels with localized kernel sizes. Thus, the region of interest by convolution is restricted within a small area, *i.e.*, the convolution operation is conducted locally, and the global structure is neglected while it contains valuable information. Considering the limitation of the convolution, how to better extract and understand the global information becomes a difficult but vital issue.

## 2.1 Background

The transformer model was created by Vaswani *et al.* in 2017[30] to collect better long-term information than recurrent neural networks and convolutional neural networks. The proposed transformer outperforms other methods and has been proven to be quite crucial in natural language processing (NLP) tasks. Furthermore, motivated by the success of transformer architecture in NLP, Dosovitskiy *et al.* [32] propose the vision transformer (ViT) for image classification and Chen *et al.* [31] design the image processing transformer (IPT) to address low-level vision tasks. Both of them obtain the best results compared to existing approaches. The achievements of the transformer in various computer vision tasks inspire us to design a network based on the transformer to solve the hyperspectral image super-resolution problem via the superior ability to capture long-term information and relationships.

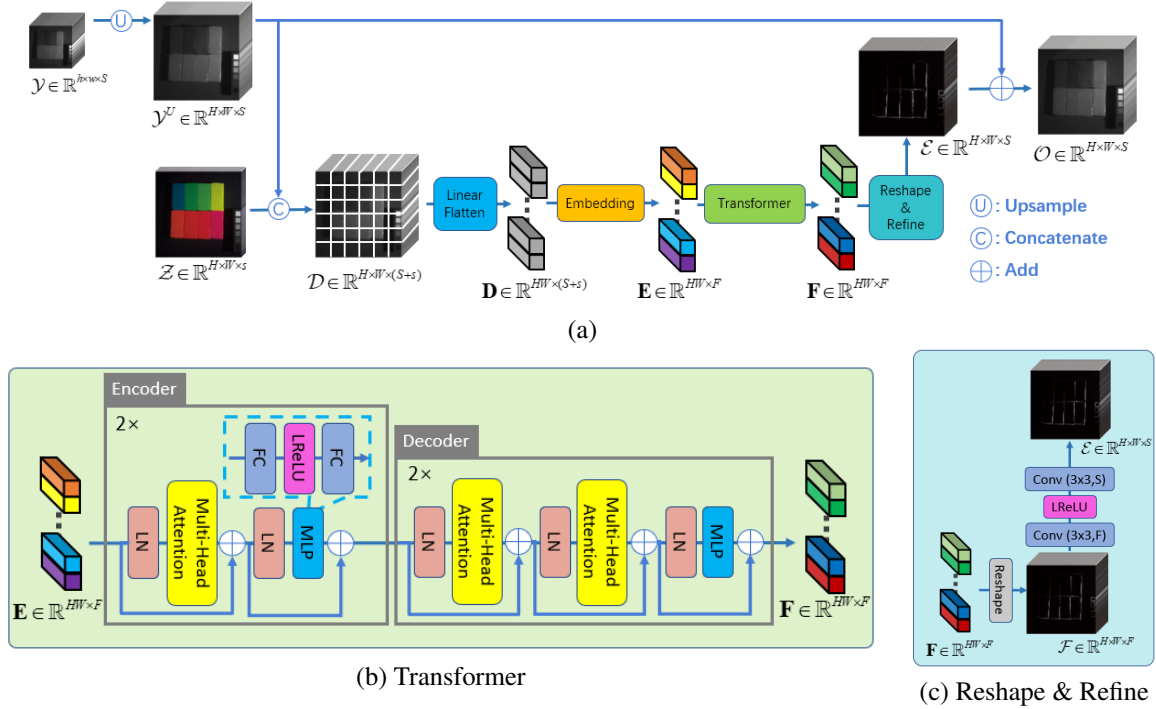


Figure 1: Overview of the proposed Fusformer network. (b) The transformer model used in the network. (c) An illustration of the reshape & refine module.

## 2.2 Proposed Method

The global information is barely used due to the limitation of the regular convolution operation with the local region of interest in the CNN architecture. Hence, we expect to use the transformer model to consider the features and information effectively and globally. The flowchart of our network structure is presented in Fig. 1. Note that the inputs of our Fusformer are the upsampled LR-HSI  $\mathcal{Y}^U \in \mathbb{R}^{H \times W \times S}$  and the HR-MSI  $\mathcal{Z} \in \mathbb{R}^{H \times W \times s}$  since the  $\mathcal{Y}^U$  holds the similar structure as the ground-truth HR-HSI  $\mathcal{X}$ .

### 2.2.1 Input of Transformer

The HR-MSI  $\mathcal{Z}$  is then concatenated with  $\mathcal{Y}^U$  along the spectral dimension. After obtaining the data cube  $\mathcal{D} \in \mathbb{R}^{H \times W \times (S+s)}$  containing the raw spectral and spatial information, we unfold the tensor  $\mathcal{D}$  to a matrix  $\mathbf{D} \in \mathbb{R}^{HW \times (S+s)}$ , due to the input's dimension requirement of the transformer model. It is worth noting that each vector in the matrix  $\mathbf{D}$  has its physical meaning *i.e.*, representing a pixel in the image with the spectral structure and corresponding spatial information. While other transformer-based methods for computer vision tasks[32, 31] reshape a small image patch into a vector directly. On the one hand, the hyperspectral image contains more spectral bands than other natural RGB images. The vector reshaped from an image patch will be too long to compute. On the other hand, we believe a vector representing pixel information instead of a patch is also suitable for our pixel-wise super-resolution problem. Hence, the transformer model is quite consistent with the characteristics of the hyperspectral image super-resolution

issue. Every pixel can be naturally represented as a vector, and the transformer architecture enables the network to discover and consider the relationships among all the pixels globally. With a simple fully connected layer, the matrix  $\mathbf{D} \in \mathbb{R}^{HW \times (S+s)}$  is then embedding to the matrix  $\mathbf{E} \in \mathbb{R}^{HW \times F}$ , where  $F$  denotes the number of feature channels ( $F = 48$  in this paper.). Next, we send the embedded patches to the transformer model, which is represented in Fig. 1-(b).

### 2.2.2 Transformer

The transformer model is the main part of our architecture which is shown in Fig. 1-(b). Here we use both the encoder and decoder part of the original transformer. As for the encoder (See the top of Fig. 1-(b)), LN indicates the layer normalization which is widely used in the transformer-based methods [30, 31, 32] for the training’s stability. Multi-head attention is the self-attention mechanism with multi-heads that enables the network to capture and consider the relationship globally. The general procedures of the self-attention mechanism are as follows.

$$\begin{aligned} \mathbf{Q} &= \mathbf{W}_q \mathbf{X}, \mathbf{K} = \mathbf{W}_k \mathbf{X}, \mathbf{V} = \mathbf{W}_v \mathbf{X}, \\ \text{Attention} &= \text{softmax}\left(\frac{\mathbf{XW}_q \mathbf{W}_k^T \mathbf{X}^T}{\sqrt{d_k}}\right) \mathbf{XW}_v \\ &= \text{softmax}\left(\frac{\mathbf{QK}^T}{\sqrt{d_k}}\right) \mathbf{V}, \end{aligned} \quad (1)$$

where  $\mathbf{W}_q$ ,  $\mathbf{W}_k$  and  $\mathbf{W}_v$  denote the corresponding weight matrices need to be trained,  $d_k$  represents the dimension of  $\mathbf{K}$  for scaling. As for the multi-head attention,  $L$  heads denotes  $L$  individual groups of  $(\mathbf{Q}_i, \mathbf{K}_i, \mathbf{V}_i)$  ( $i = 1, 2, \dots, L$ ) with  $L$  attention values. Furthermore, softmax gives attention values from 0 to 1 which differentiate levels of importance in  $\mathbf{V}$ . The whole algorithm of the encoder can be described as follows.

$$\begin{aligned} \mathbf{X}' &= \text{MHA}(\text{LN}(\mathbf{X})) \\ \mathbf{X} &= \mathbf{X} + \mathbf{X}' \\ \mathbf{X}' &= \text{MLP}(\text{LN}(\mathbf{X})) \\ \mathbf{X} &= \mathbf{X} + \mathbf{X}', \end{aligned} \quad (2)$$

where LN represents the layer normalization, MHA denotes the multi-head attention module and the MLP defines the multi-layer perception plotted in Fig. 1-(c). Similarly, the decoder can be described as follows.

$$\begin{aligned} \mathbf{X}' &= \text{MHA}(\text{LN}(\mathbf{X})) \\ \mathbf{X} &= \mathbf{X} + \mathbf{X}' \\ \mathbf{X}' &= \text{MHA}(\text{LN}(\mathbf{X})) \\ \mathbf{X} &= \mathbf{X} + \mathbf{X}' \\ \mathbf{X}' &= \text{MLP}(\text{LN}(\mathbf{X})) \\ \mathbf{X} &= \mathbf{X} + \mathbf{X}' \end{aligned} \quad (3)$$

After getting the learned features  $\mathbf{F} \in \mathbb{R}^{HW \times F}$ , we reshape it back to a 3D tensor  $\mathcal{F} \in \mathbb{R}^{H \times W \times F}$  and then feed it to a refine module for the desired residual  $\mathcal{E} \in \mathbb{R}^{H \times W \times S}$ . Finally, the output  $\mathcal{O}$  is obtained by adding the upsampled LR-HSI  $\mathcal{Y}^U$  and learned residual  $\mathcal{E}$ .

## 3 Experiment Results

To verify the effectiveness of our proposed Fusformer, we compare with classic and state-of-the-art 1) traditional approaches: FUSE [33], GLP-HS [7], CSTF [9] and CNN-FUS [10]. 2) deep learning-based approaches: SSRNet [28], ResTFNet [29], MHF-Net [19] and HSRnet [34] on two different hyperspectral image datasets *i.e.*, CAVE dataset [35] and Harvard dataset [36]. Both of them contain hyperspectral images with 31 spectral channels. Images of CAVE dataset are with a size of  $512 \times 512$ , while images of Harvard dataset are cropped with the spatial size of  $1000 \times 1000$ . 20 images from CAVE dataset are selected for training, 11 images from CAVE dataset, and 10 images from Harvard dataset are for testing. Note that all the training images are from the CAVE dataset. The images from the Harvard dataset thus can be used for the generalization test, which is quite crucial for deep learning-based methods.

Tab. 1 and 2 list the quantitative comparisons in CAVE and Harvard datasets. Our proposed Fusformer obtains the best results on almost every QI and involves only 0.1 million parameters, making our network more practical. We also show visual presentation and corresponding absolute residual maps of two samples selected from CAVE and Harvard dataset in Fig. 2. It is obvious that our approach still outperforms other methods and the residuals are the darkest.

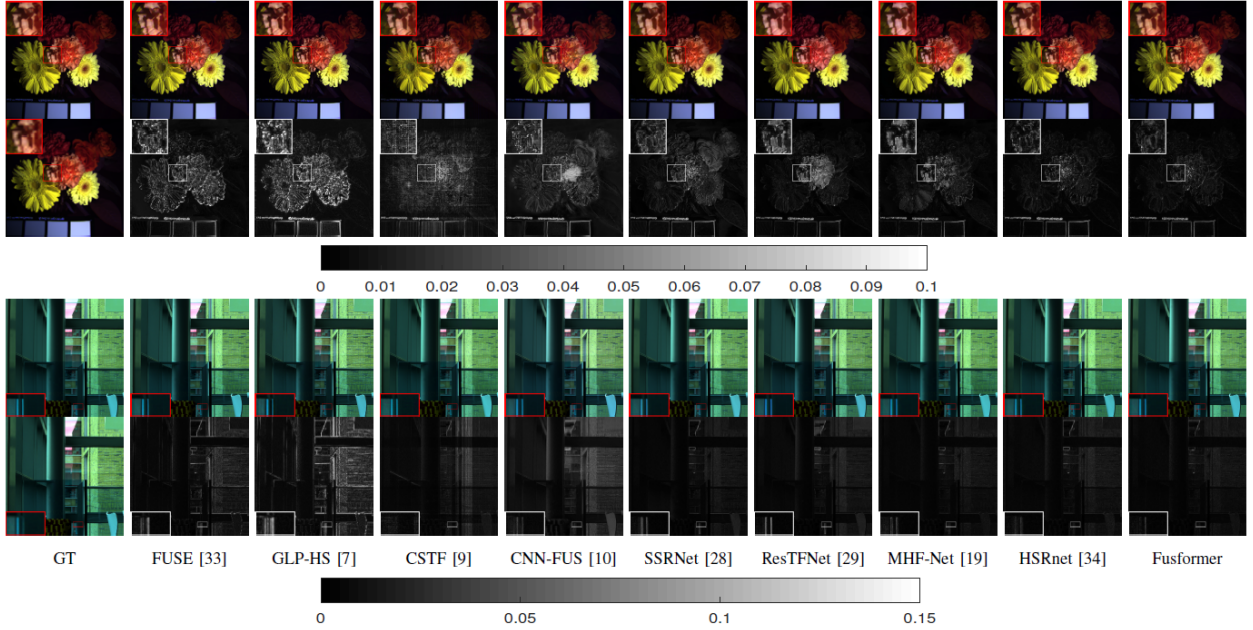


Figure 2: The first column: the true pseudo-color images from the CAVE and Harvard dataset and the corresponding LR-HSI images of *feathers* (R-31, G-24, B-2) (1st-2nd rows) and *window* (R-29, G-21, B-13) (3th-4th rows). The 2nd-8th columns: the true pseudo-color fused products and the corresponding residuals for the different methods in the benchmark pointing out some close-ups to facilitate the visual analysis.

Table 1: Average QIs of the results on 11 testing images from the CAVE dataset and the corresponding number of parameters. The best values are highlighted in boldface, the second best values are highlighted in underline, while M indicates a million.

Method	PSNR	SAM	ERGAS	SSIM	# parameters
FUSE[33]	39.72	5.83	4.18	0.975	/
GLP-HS[7]	37.81	5.36	4.66	0.972	/
CSTF[9]	42.14	9.92	3.08	0.964	/
CNN-FUS[10]	42.66	6.44	2.95	0.982	/
SSRNet[28]	45.28	4.72	2.06	0.990	<b>0.03M</b>
ResTFNet[29]	45.35	3.76	1.98	<u>0.993</u>	2.26M
MHF-Net[19]	46.32	4.33	1.74	0.992	3.63M
HSRnet [34]	<u>47.82</u>	<u>2.66</u>	<u>1.34</u>	<b>0.995</b>	1.90M
Fusformer	<b>48.56</b>	<b>2.52</b>	<b>1.30</b>	<b>0.995</b>	<u>0.10M</u>
Best value	$+\infty$	0	0	1	0

### 3.1 Generalization Ability

Furthermore, deep learning-based methods usually perform poorly on examples that differ from the training dataset. Hence, the generalization ability of deep learning-based methods is quite crucial. However, our Fusformer is still satisfying, and only the ERGAS is not the smallest. The generalization performance of HSRnet is close to the proposed Fusformer, but its involved parameters are much more than Fusformer.

### 3.2 Ablation Study

Our Fusformer is excepted for learning the residuals between the upsampled LR-HSI  $\mathcal{Y}^U$  and ground-truth  $\mathcal{X}$  instead of reconstructing the whole HSI. We conduct a simple experiment to verify the residual learning strategy (RLS) *i.e.*, adding the upsampled LR-HSI  $\mathcal{Y}^U$  to the outcome learned by the network. Tab. 3 records the results of the architecture with or without the RLS. It is clear that adding the upsampled LR-HSI  $\mathcal{Y}^U$  is quite vital for the network. The rough information of  $\mathcal{Y}^U$  helps the network to boost the performance and strengthen the stability.

Table 2: Average QIs of the results for 10 testing images from the Harvard dataset and the corresponding number of parameters. The best values are highlighted in boldface, the second best values are highlighted in underline, while M indicates a million.

Method	PSNR	SAM	ERGAS	SSIM	# parameters
FUSE[33]	42.06	<u>3.23</u>	3.14	0.977	/
GLP-HS[7]	40.14	3.52	3.74	0.966	/
CSTF[9]	42.97	3.30	<b>2.43</b>	0.972	/
CNN-FUS[10]	43.61	3.32	2.78	<u>0.978</u>	/
SSRNet[28]	39.87	5.40	5.44	<u>0.963</u>	<b>0.03M</b>
ResTFNet[29]	38.39	5.85	6.98	0.957	2.26M
MHF-Net[19]	40.37	4.64	24.17	0.966	3.63M
HSRnet[34]	<u>44.28</u>	<b>2.66</b>	<u>2.45</u>	<b>0.984</b>	1.90M
Fusformer	<b>44.42</b>	<b>2.66</b>	<u>2.48</u>	<b>0.984</b>	<u>0.10M</u>
Best value	$+\infty$	0	0	1	0

Table 3: Average QIs and related standard deviations of the results on the CAVE dataset using the proposed method with and without the residual learning strategy. The best values are highlighted in boldface.

Method	PSNR	SAM	ERGAS	SSIM
W/o RLS	42.71 $\pm$ 7.82	3.29 $\pm$ 1.24	4.48 $\pm$ 7.43	0.984 $\pm$ 0.02
Fusformer	<b>48.56<math>\pm</math>3.03</b>	<b>2.52<math>\pm</math>0.83</b>	<b>1.30<math>\pm</math>0.86</b>	<b>0.995<math>\pm</math>0.00</b>

## 4 Conclusion

In this work, a transformer-based network architecture called Fusformer is proposed. Compared with previous CNN-based methods, our method can consider the global information instead of the local information in a receptive field with a limited kernel size. This is the first time adopting the transformer model in the hyperspectral image super-resolution issue to the best of our knowledge. Our method is simple yet effective and contains few parameters. Future researches can further exploit the potential base on our proposed framework.

## 5 Acknowledge

The work is supported by National Natural Science Foundation of China grants 12001446, 61702083, 12171072 and 61876203, and the Fundamental Research Funds for the Central Universities JBK2001011.

## References

- [1] Renwei Dian, Shutao Li, Bin Sun, and Anjing Guo. Recent advances and new guidelines on hyperspectral and multispectral image fusion. *Information Fusion*, 69:40–51, 2020.
- [2] Tai-Xiang Jiang, Michael K Ng, Xi-Le Zhao, and Ting-Zhu Huang. Framelet representation of tensor nuclear norm for third-order tensor completion. *IEEE Transactions on Image Processing*, 29:7233–7244, 2020.
- [3] Yang Xu, Zebin Wu, Jocelyn Chanussot, and Zhihui Wei. Hyperspectral images super-resolution via learning high-order coupled tensor ring representation. *IEEE Transactions on Neural Networks and Learning Systems*, 31(11):4747–4760, 2020.
- [4] W. Hu, D. Tao, W. Zhang, Y. Xie, and Y. Yang. The twist tensor nuclear norm for video completion. *IEEE Transactions on Neural Networks and Learning Systems*, 28(12):2961–2973, 2017.
- [5] Tai-Xiang Jiang, Ting-Zhu Huang, Xi-Le Zhao, Liang-Jian Deng, and Yao Wang. A novel tensor-based video rain streaks removal approach via utilizing discriminatively intrinsic priors. In *Proceedings of the IEEE Conference on Computer Vision and Pattern Recognition (CVPR)*, pages 2818–2827, 2017.
- [6] Xiaolin Han, Jiqiang Luo, Jing Yu, and Weidong Sun. Hyperspectral image fusion based on non-factorization sparse representation and error matrix estimation. In *Proceedings of the IEEE Global Conference on Signal and Information Processing (GlobalSIP)*, pages 1155–1159, 2017.
- [7] Massimo Selva, Bruno Aiuzzi, Francesco Butera, Leandro Chiarantini, and Stefano Baronti. Hyper-sharpening: A first approach on SIM-GA data. *IEEE Journal of Selected Topics in Applied Earth Observations and Remote Sensing*, 8(6):3008–3024, 2015.

- [8] T. Akgun, Y. Altunbasak, and R. M. Mersereau. Super-resolution reconstruction of hyperspectral images. *IEEE Transactions on Image Processing*, 14(11):1860–1875, 2005.
- [9] Shutao Li, Renwei Dian, Leyuan Fang, and Jose M Bioucasdias. Fusing hyperspectral and multispectral images via coupled sparse tensor factorization. *IEEE Transactions on Image Processing*, 27(8):4118–4130, 2018.
- [10] R. Dian, S. Li, and X. Kang. Regularizing hyperspectral and multispectral image fusion by cnn denoiser. *IEEE Transactions on Neural Networks and Learning Systems*, 32(3):1124–1135, 2021.
- [11] Ting Xu, Ting-Zhu Huang, Liang-Jian Deng, Xi-Le Zhao, and Jie Huang. Hyperspectral image superresolution using unidirectional total variation with tucker decomposition. *IEEE Journal of Selected Topics in Applied Earth Observations and Remote Sensing*, 13:4381–4398, 2020.
- [12] Zhiwei Pan and Huiliang Shen. Multispectral image super-resolution via RGB image fusion and radiometric calibration. *IEEE Transactions on Image Processing*, 28(4):1783–1797, 2019.
- [13] Renwei Dian and Shutao Li. Hyperspectral image super-resolution via subspace-based low tensor multi-rank regularization. *IEEE Transactions on Image Processing*, 28(10):5135–5146, 2019.
- [14] Renwei Dian, Shutao Li, and Leyuan Fang. Learning a low tensor-train rank representation for hyperspectral image super-resolution. *IEEE Transactions on Neural Networks and Learning Systems*, 30(9):2672–2683, 2019.
- [15] Zhong-Cheng Wu, Ting-Zhu Huang, Liang-Jian Deng, Gemine Vivone, Jia-Qing Miao, Jin-Fan Hu, and Xi-Le Zhao. A new variational approach based on proximal deep injection and gradient intensity similarity for spatio-spectral image fusion. *IEEE Journal of Selected Topics in Applied Earth Observations and Remote Sensing*, 13:6277–6290, 2020.
- [16] Xueyang Fu, Wu Wang, Yue Huang, Xinghao Ding, and John Paisley. Deep multiscale detail networks for multiband spectral image sharpening. *IEEE Transactions on Neural Networks and Learning Systems*, 32(5):2090–2104, 2021.
- [17] Liang-Jian Deng, Gemine Vivone, Weihong Guo, Mauro Dalla Mura, and Jocelyn Chanussot. A variational pansharpening approach based on reproducible kernel hilbert space and heaviside function. *IEEE Transactions on Image Processing*, 27(9):4330–4344, 2018.
- [18] Liang-Jian Deng, Minyu Feng, and Xue-Cheng Tai. The fusion of panchromatic and multispectral remote sensing images via tensor-based sparse modeling and hyper-laplacian prior. *Information Fusion*, 52:76–89, 2019.
- [19] Qi Xie, Minghao Zhou, Qian Zhao, Zongben Xu, and Deyu Meng. MHF-Net: An interpretable deep network for multispectral and hyperspectral image fusion. *IEEE Transactions on Pattern Analysis and Machine Intelligence*, 2020. DOI:10.1109/TPAMI.2020.3015691.
- [20] Renwei Dian, Shutao Li, Anjing Guo, and Leyuan Fang. Deep hyperspectral image sharpening. *IEEE Transactions on Neural Networks and Learning Systems*, 29(11):5345–5355, 2018.
- [21] Zhenfeng Shao and Jiajun Cai. Remote sensing image fusion with deep convolutional neural network. *IEEE Journal of Selected Topics in Applied Earth Observations and Remote Sensing*, 11(5):1656–1669, 2018.
- [22] Yunsong Li, Jing Hu, Xi Zhao, Weiyang Xie, and Jiaojiao Li. Hyperspectral image super-resolution using deep convolutional neural network. *Neurocomputing*, 266:29–41, 2017.
- [23] Sergio Vitale. A CNN-based pansharpening method with perceptual loss. In *Proceedings of the IEEE International Geoscience and Remote Sensing Symposium (IGARSS)*, pages 3105–3108, 2019.
- [24] X. Han, j. Yu, J. Luo, and W. Sun. Hyperspectral and multispectral image fusion using cluster-based multi-branch BP neural networks. *Remote Sensing*, 11(10):1173, 2019.
- [25] Y. Liu, X. Chen, Z. Wang, Z. Wang, R. Ward, and X. Wang. Deep learning for pixel-level image fusion: Recent advances and future prospects. *Information Fusion*, 42:158–173, 2018.
- [26] W. Huang, L. Xiao, Z. Wei, H. Liu, and S. Tang. A new pan-sharpening method with deep neural networks. *IEEE Geoscience and Remote Sensing Letters*, 12(5):1037–1041, 2015.
- [27] X. Y. Liu, Y. Wang, and Q. Liu. PSGAN: a generative adversarial network for remote sensing image pansharpening. In *Proceedings of the IEEE International Conference on Image Processing (ICIP)*, pages 873–877, 2018.
- [28] X. Zhang, W. Huang, Q. Wang, and X. Li. SSR-NET: Spatial-spectral reconstruction network for hyperspectral and multispectral image fusion. *IEEE Transactions on Geoscience and Remote Sensing*, 59(7):5953–5965, 2021.
- [29] Xiangyu Liu, Qingjie Liu, and Yunhong Wang. Remote sensing image fusion based on two-stream fusion network. *Information Fusion*, 2020. DOI:10.1016/j.inffus.2019.07.010.

- [30] Ashish Vaswani, Noam Shazeer, Niki Parmar, Jakob Uszkoreit, Llion Jones, Aidan N Gomez, Łukasz Kaiser, and Illia Polosukhin. Attention is all you need. In *Advances in Neural Information Processing Systems (NeurIPS)*, pages 5998–6008, 2017.
- [31] Hanqing Chen, Yunhe Wang, Tianyu Guo, Chang Xu, Yiping Deng, Zhenhua Liu, Siwei Ma, Chunjing Xu, Chao Xu, and Wen Gao. Pre-trained image processing transformer. In *Proceedings of the IEEE Conference on Computer Vision and Pattern Recognition (CVPR)*, pages 12299–12310, 2021.
- [32] Alexey Dosovitskiy, Lucas Beyer, Alexander Kolesnikov, Dirk Weissenborn, Xiaohua Zhai, Thomas Unterthiner, Mostafa Dehghani, Matthias Minderer, Georg Heigold, Sylvain Gelly, et al. An image is worth 16x16 words: Transformers for image recognition at scale. *arXiv preprint arXiv:2010.11929*, 2020.
- [33] Qi Wei, Nicolas Dobigeon, and Jean-Yves Tourneret. Fast fusion of multi-band images based on solving a Sylvester equation. *IEEE Transactions on Image Processing*, 24(11):4109–4121, 2015.
- [34] Jin-Fan Hu, Ting-Zhu Huang, Liang-Jian Deng, Tai-Xiang Jiang, Gemine Vivone, and Jocelyn Chanussot. Hyperspectral image super-resolution via deep spatio-spectral attention convolutional neural networks. *IEEE Transactions on Neural Networks and Learning Systems*, 2021. DOI:10.1109/TNNLS.2021.3084682.
- [35] Fumihito Yasuma, Tomoo Mitsunaga, Daisuke Iso, and Shree Nayar. Generalized assorted pixel camera: postcapture control of resolution, dynamic range, and spectrum. *IEEE Transactions on Image Processing*, 19(9):2241–2253, 2010.
- [36] Ayan Chakrabarti and Todd Zickler. Statistics of real-world hyperspectral images. In *Proceedings of the IEEE Conference on Computer Vision and Pattern Recognition (CVPR)*, pages 193–200, 2011.